Indian Journal of Chemistry
Vol. 59A, July 2020, pp. 929-938

Experimental and theoretical investigations on the host-guest interaction of diphenylamine with p-sulfonatocalix**[**4**]**arene

Chokalingam Saravanan[a], Ramesh Kumar Chitumalla[b], Rathinam Yuvakumar[c], Poovan Shanmugavelan[d], Paulpandian Muthu Mareeswaran [a,]* & Joonkyung Jang [b,]*

[a]Department of Industrial Chemistry, Alagappa University, Karaikudi, Tamilnadu, India

[b]Department of Nanoenergy Engineering, Pusan National University, Busan 46241, Republic of Korea

[c]Department of Physics, Alagappa University, Karaikudi, Tamilnadu, India

[d]Department of Chemistry, School of Sciences, Tamilnadu Open University, Chennai, Tamilnadu, India

E-mail: mareeswaran@alagappauniversity.ac.in, muthumareeswaran@gmail.com, jkjang@pusan.ac.kr

Received 08 January 2020; revised and accepted 13 May 2020

The intermolecular interaction between diphenylamine (DPA) and p-sulfonatocalix[4]arene (p-SC4) is studied by experimental and computational techniques. The 1:1 stoichiometry of the inclusion complex is deduced from fluorescence titration using Job's method. The tendency of binding of DPA with p-SC4 is analyzed from emission, excited state lifetime and cyclic voltammetry techniques. The binding constant values acquired from all the titrations are around 10^3–10^4 L/mol, reveals the effective binding. The structural interactions and mode of binding of the supramolecular complex are explained by ^{1}H NMR and ROESY spectral studies. The molecular association of DPA with p-SC4 is confirmed by quantum chemical simulations. The higher complexation energy (-76.94 kJ/mol) declares the existence of strong binding between DPA and p-SC4.

Keywords: p-Sulfonatocalix[4]arene, Diphenylamine, Spectral titrations, Electrochemical study, Theoretical interpretation, Complexation energy

Calixarenes are macrocyclic oligomers having flexible template for building numerous structures with exciting host-guest properties, recognized as the third generation organic supramolecular host compounds after cyclodextrins and crown ethers[1-3]. Calixarenes are attractive molecular receptors with accessible chemical modifications to adopt organic molecules inside the cavity[4]. The basic calixarenes structures have limited functional applications because of their poor water solubility. Enormous amount of strategies are executed to improve the water solubility of basic calixarene structures by means of upper and lower rim modifications to impart efficient molecular recognition properties towards bio-system[5,6]. Most of the synthetic modifications of calixarenes are aimed at the recognition and delivery of larger drug molecules[7-10]. Water soluble acid derivatives of calixarenes, such as *p*-sulfonato-, *o*-phosphonato-, *o*-alkylcarboxylato-calixarenes are envisaged as suitable receptors for biologically important molecules[11,12]. The *para*-sulfonatocalix[4]arene (p-SC4), is a prominent water soluble anionic calixarene derivative in the field of molecular recognition[13,14]. The p-SC4 provides three dimensional, open, flexible, π-rich cavity and anchoring point by means of sulfonate groups to accommodate a variety of metals, organic cations and neutral organic molecules in aqueous medium[15-17]. The diverse interactions such as ionic, hydrophilic as well as hydrophobic nature are exclusive properties of p-SC4[18]. In aqueous media, the hydrophobic and π-π stacking interactions are the driving forces for the guest incorporation into the p-SC4 cavity[19,12,20]. The recognition of fluorophores by host molecules such as p-SC4 is a wide area of research in supramolecular as well as photochemistry[21-24]. The strategy of changing the fluorescent properties of fluorophores upon complexation leads to several applications from sensors to site selective drug delivery[25-30].

Diphenylamine (DPA) is mainly used as a post-harvest anti-fungal agent and is used to protect scald formation in fruits like apple, pear during storage[31,32]. DPA is a commonly used stabilizer in multi-base propellants, nitrocellulose containing explosives, antioxidants for various polymers, elastomers and

condensates for the insulation of rubber[33]. The DPA and its derivatives, are commonly applied in the manufacturing of dyes, photography chemicals, pharmaceutical processes[31]. It has biological applications, such as fungicidal activity, insecticidal, acaricidal, and rodenticidal activity[34,35]. Fluorimetric photochemical conversion of DPA to carbazole in aerated aqueous and β-Cyclodextrin environments has been investigated by Chattopadhyay group[36,37]. The DPA incorporated polymer electrolyte material is a promising one for dye-sensitized solar cells, which improves the stability by decreasing the sublimation of I_2 to a considerable extent[38]. The inclusion complex and proton transfer efficiency of diphenylamine with β-cyclodextrin in the aqueous medium have been reported by M. Swaminathan group[39-41]. The photophysical and electrochemical behavior of DPA with β-cyclodextrin have been reported by Srinivasan et al[37]. However, the photochemical and electrochemical properties of DPA in the presence of highly polar anionic guest molecule like p-SC4 is not reported yet. The DPA is having a secondary amine group as well as phenyl groups with propensity of binding with hydrophobic cavity as well as hydrophilic upper and lower rims. Herein, we report the supramolecular interaction between DPA and p-SC4, through spectrofluorimetric, electrochemical, NMR analysis and computational studies.

Materials and Methods

Diphenylamine (DPA) was purchased from Avra synthesis Pvt. Ltd, Hyderabad, India. The p-SC4 was synthesized by the procedure from the earlier reports[17,13,42]. Sulfuric acid and HPLC grade acetonitrile was procured from Sisco Research Laboratories Pvt. Ltd, Mumbai, India. Acetonitrile and Millipore water were used as solvents to prepare the stock and the sample solutions. The whole experiments were carried out at room temperature (~25 ºC) without use of buffer solutions. The p-SC4 exhibits pH~8 in aqueous medium.

Binding constant calculation from fluorescence spectroscopy

The fluorescence spectra of DPA (1×10^{-6} mol/L) were recorded in the absence and in the presence of increasing concentration of p-SC4 (1×10^{-6} mol/L to 9×10^{-5} mol/L) using Agilent spectrophotometer. The binding constant value is evaluated based on the increase of emission intensity of DPA with the increasing concentration of p-SC4. We have calculated the binding constant value from the modified Benesi–Hildebrand equation,

$$\frac{I_0}{I-I_0} = b(a-b)\left[\frac{1}{K_a[H]} + 1\right] \quad \ldots (1)$$

where, I_0 is the fluorescence intensity of DPA without p-SC4, I is the fluorescence intensity of DPA with various concentrations of p-SC4, [H] is the concentration of p-SC4, K_a is the binding constant, a and b are constants. The plot of $I_0/(I-I_0)$ versus the inverse of the concentration of p-SC4 gave a straight line. The binding constant K_a was calculated from the slope of the straight line. The binding stoichiometry was determined using the Job's plot method. The mixture of p-SC4 (varied from 1×10^{-6} mol/L to 9×10^{-6} mol/L) and DPA (varied from 1×10^{-6} mol/L to 9×10^{-6} mol/L) were prepared and the emission measurements are carried out. Plotting mole fraction versus changes in fluorescence intensity gives the stoichiometric ratio for DPA/p-SC4 complex.

Calculation of free energy change from emission titration

The host-guest complex formation was also evaluated by the thermodynamic parameter i.e. free energy change of a reaction. The ΔG value was calculated from the binding constant value using the following equation,

$$\Delta G = -RT\, LnK_a \quad \ldots (2)$$

where, ΔG is the free energy change of the reaction, R is gas constant, T is temperature and K_a is binding constant value.

Fluorescence lifetime study

The excited state fluorescence lifetime of DPA with p-SC4 was measured using time correlated single photon counting method (TCSPC) in HORIBA JOBIN-VYON data station. The pulse light-emitting diodes were the dominant light sources for TCSPC[43]. In this experiment, 280 nm pulse-LED was the light source to excite the molecule. The DPA molecule, concentration is fixed at 1×10^{-4} mol/L and concentration of p-SC4 is varied from 0.5×10^{-4} mol/L to 2×10^{-4} mol/L. The fluorescence lifetime of DPA with p-SC4 is calculated by plotting decay versus time from the system generated data.

Electrochemical measurements

The host-guest titration study was carried out electrochemically, using cyclic voltammetry technique on a CHI604D electrochemical analyzer. Three electrode systems were used, glassy carbon (GC) as working electrode, silver-silver chloride as reference electrode, and platinum rod as counter

electrode. The concentration of DPA (10 mL, 10^{-3} mol/L) was fixed and the concentration of p-SC4 (2-10 mL of 10^{-3} mol/L) was increased and vice versa. The mixture was allowed to stir for 2 min, after each 2 mL addition of host or guest. The binding constant was calculated from the following Benesi–Hildebrand equation[37,44],

$$\frac{1}{I_{HG}-I_G} = \frac{1}{\Delta I} + 1/(K_a[DPA]_0 \Delta I[p-SC4]_0 \quad \ldots (3)$$

where, I_G is the oxidation peak current of DPA without p-SC4, I_{HG} is oxidation peak current of the DPA with p-SC4, and I_{HG}-I_G is the oxidation peak current of the DPA/p-SC4 complex and the DPA alone, ΔI is the difference between the molar peak current coefficient of the complex and the DPA. $[DPA]_0$ and $[p\text{-}SC4]_0$ are the initial concentrations of DPA and p-SC4, respectively. The plot of $1/(I_{HG}-I_G)$ versus 1/[p-SC4] gave a straight line. From the slope value of the straight line, we have calculated the binding constant. The free energy change value was calculated from the binding constant value K_a by using Eqn 2.

NMR analysis

The host-guest interaction between DPA and p-SC4 was studied by NMR spectral titration using Bruker 500 MHz spectrometer. The mixture of acetonitrile-deuterium oxide (1:3) was used as solvent for ^{1}H NMR titration and rotating frame nuclear Overhauser effect spectroscopy (ROESY) spectral studies.

Computational methods

All the calculations reported in this work were performed by Gaussian 09 quantum chemical software[45] within the framework of density functional theory (DFT). The optimized structures of the host (p-SC4) and guest (DPA) molecules were used to calculate the complex structure. The optimized geometries are then subjected to the vibrational frequency analysis to ensure no imaginary frequencies on the potential energy surface. The most stable host-guest complex was used to obtain the frontier molecular orbitals (FMOs) to study the charge transfer phenomenon. The simulations were performed at the M06-2X/6-31G(d) level of theory[46]. The employed Minnesota hybrid exchange-correlation functional (with 56% Hartree-Fock contribution) has been widely used previously for this type of interaction studies. All the calculations were performed in the vacuum without imposing any symmetry constraints.

Results and Discussion

The supramolecular complexation of DPA with p-SC4 was investigated by emission, excited state lifetime, cyclic voltammetry, ^{1}H NMR titrations and computational studies. The structures of DPA and p-SC4 are given in Scheme 1.

Fluorescence titration

Fluorescence spectroscopy is a highly sensitive and suitable technique to evaluate the host-guest complexation between DPA and p-SC4, since the host molecule p-SC4 does not exhibit any fluorescence behavior. The emission spectrum of DPA is shown in Fig. S1 (Supporting Data). The emission maximum of DPA is observed at 385 nm upon excitation at 285 nm. The concentration of DPA is fixed at 1×10^{-6} mol/L and the concentration of p-SC4 varied and the emission measurements are carried out. The emission intensity of DPA increases after the addition of increasing concentration of p-SC4 is given in Fig. 1. The binding constant value is calculated from the enhancement in the fluorescence intensity of DPA using Eqn 1. The binding constant value of DPA with p-SC4 complex is 1.46×10^4 L/mol. The Benesi–Hildebrand plot is shown in Fig. S2. The binding ratio is calculated using Job's method. The Job's plot is given in Fig. 2. The 0.5 mole fraction indicates the 1:1 stoichiometry of the p-SC4 /DPA complex. The ΔG value is calculated using Eqn 2. The ΔG of DPA in the presence of increasing concentration of p-SC4 is -24.1 kJ/mol. The negative ΔG value represents the spontaneous interaction upon inclusion. The p-SC4

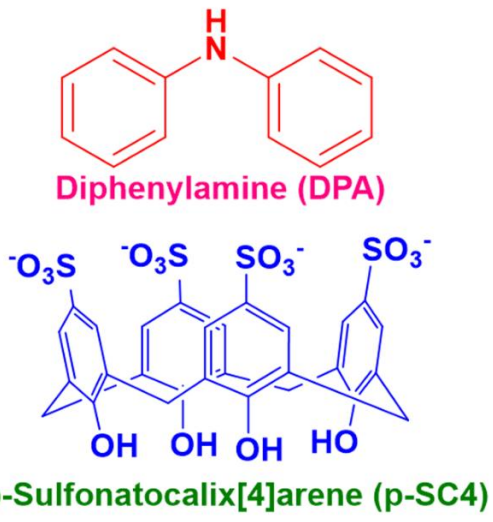

Scheme 1 — Molecular structures of diphenylamine and p-sulfonatocalix[4]arene.

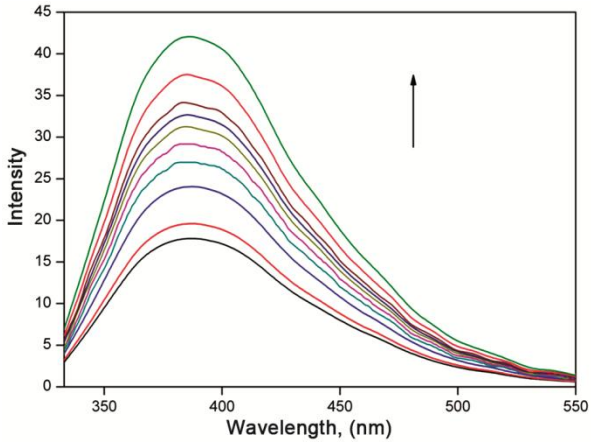

Fig. 1 — Emission spectra of DPA (1 × 10^{-6} mol/L) in the presence of varying addition of p-SC4 (excited at 285 nm).

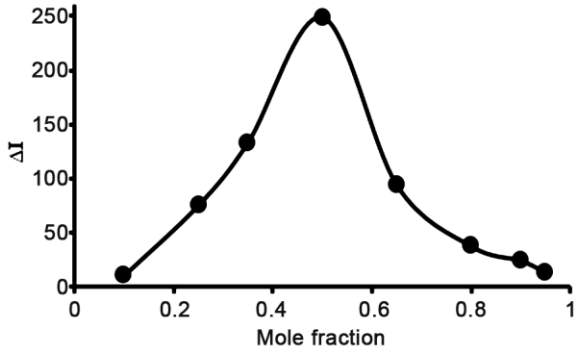

Fig. 2 — Job's plot of DPA/p-SC4 complex from fluorescence titration.

has ability to sequester its own counter ions (Na^+), resulting in a decrease of the host available for complexation of an external guest on increasing the calixarene concentration are reported by Garcia-Rio et al. and Nau et al.[18]. The competitive binding of p-SC4 with Na^+ is not comparable with organic guest molecules, because of the weak counter ion binding possess low binding constant values[47-49,18]. Also, both p-SC4 and counter ion have no fluorescent properties, the results observed from the spectroscopic titration is only due to the change in the fluorescence of DPA molecules upon encapsulation of p-SC4.

Excited state lifetime

The excited state lifetime of DPA is 740.86 ps in aqueous solution. Keeping the concentration of DPA constant at 1 × 10^{-4} mol/L, varying the concentration of p-SC4 from 0.5 × 10^{-4} mol/L to 2 × 10^{-4} mol/L, excited state lifetime is measured for these samples. The lifetime of DPA is increased with the increasing concentration of p-SC4.The decay plot is shown

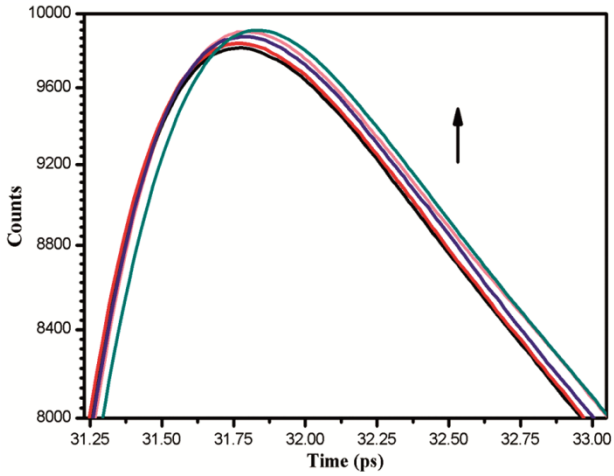

Fig. 3 — Excited state lifetime of DPA (1 × 10^{-4} mol/L) in the presence of increasing addition of p-SC4 (0.5 × 10^{-4} mol/L to 2 × 10^{-4} mol/L) (excited at 285 nm).

Table 1 — Excited state lifetime changes of DPA with the addition of increasing concentration of p-SC4

S. No	Concentration of p-SC4 (mol/L)	Lifetime (τ) (ps)
1	Without p-SC4	740.86
2	0.5 × 10^{-4}	753.78
3	1 × 10^{-4}	756.84
4	1.5 × 10^{-4}	761.50
5	2 × 10^{-4}	775.13

in Fig. 3 and the lifetime data is given in Table. 1. The changes observed in the lifetime of DPA in the presence of p-SC4 indicate the stable complex formation.

Electrochemical analysis

The concentration of DPA is kept constant and the experiment is carried out at the scan rate of 50 mV in aqueous medium. A single oxidation peak is observed at 0.52 V, represents the formation of diphenylamine cation radical. The reduction peak appeared at 0.25 V is due to the DPA cation radical reduction (Fig. S3)[50,51]. The increase in anodic peak current and the shift in the peak potential towards negative side upon adding the p-SC4, indicate the complexation behavior (Fig. 4). A new oxidation peak is developed at around 0.75 V, while introducing p-SC4 first due to the one electron oxidation of diphenylamine cation radical[52,53]. When the amount of p-SC4 is increased subsequently the anodic peak current at 0.75 V is decreased, due to the DPA accommodation. The oxidation of amine group to produce cation radical is suppressed by means of formation of intermolecular hydrogen bonding of hydrogen of secondary amine

group with oxygen of sulfonate group of p-SC4. The hydrogen bond formation is explained using the computational technique in the subsequent section. The detailed changes are given in Table 2. A small hump has appeared at 0.9 V from p-SC4 until the 1:1 ratio is reached. The DPA polymerization is inhibited while increasing the concentration of p-SC4. The binding constant value is 3.81×10^3 L/mol. The Benesi–Hildebrand plot of DPA/p-SC4 complex is shown in Fig. S5. The ΔG value obtained is -20.7 kJ/mol, denotes the complexation is spontaneous.

Similarly, by keeping the p-SC4 concentration constant, the concentration of DPA is varied and the experiment is carried out at the same scan rate. A wave like oxidation peak observed at 0.81 V, belongs to phenolate ion oxidation of p-SC4 (Fig. S4)[54,55]. There is an immediate peak potential shift towards negative side upon complexation with DPA is observed. The increase of concentration of DPA enhances the oxidation peak current of p-SC4 through complexation. The results obtained from cyclic voltammetry are similar to our previous reports of p-SC4 with different organic molecules[26,27]. The oxidation peak at 0.38 V has also appeared after the addition of DPA, which indicates the DPA presence (Fig. 5). The peak values are displayed in Table 3. The peak at 0.72 V for the DPA mono cation, are merged with the p-SC4, while 1:1 ratio is reached. The binding constant value obtained is 1.1×10^3 L/mol, calculated from Eqn 3. The Benesi–Hildebrand plot is given in Fig. S6. The ΔG value from Eqn 2 is -17.6 kJ/mol suggests that the inclusion is spontaneous. The obtained binding constant values

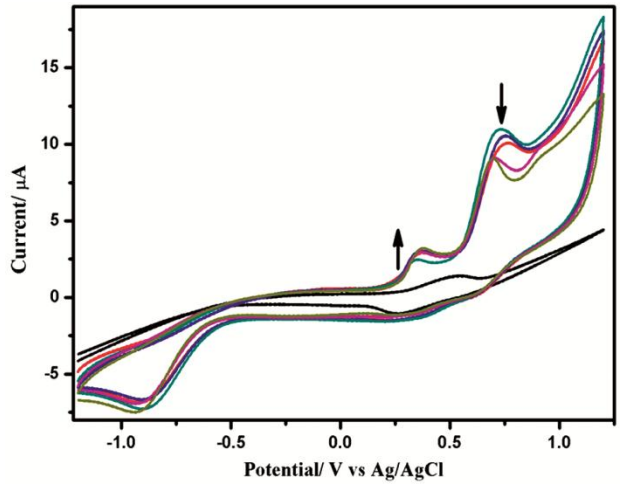

Fig. 4 — Cyclic voltammogram of DPA (10 mL, 10^{-3} mol/L) in the presence of increasing amount of p-SC4 (2 – 10 mL, 10^{-3} mol/L) (scan rate is 50 mV/s).

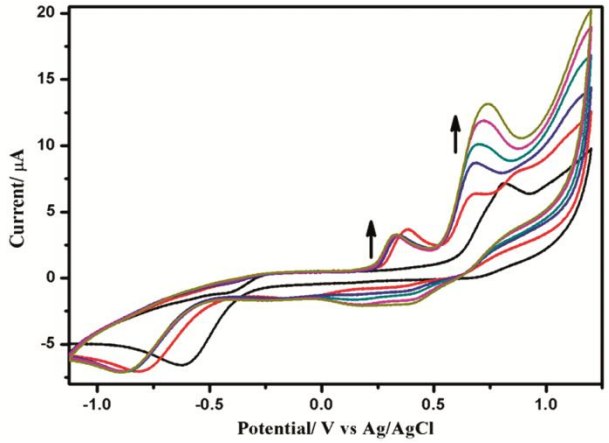

Fig. 5 — Cyclic voltammogram of p-SC4 (10 mL, 10^{-3} mol/L) in the presence of increasing concentration of DPA (2 – 10 mL, 10^{-3} mol/L) (scan rate is 50 mV/s).

Table 2 — CV of DPA with varying concentration of p-SC4 at the scan rate of 50 mV/s

S. No	Concentration of p-SC4 (mL, 10^{-3}mol/L)	Epa_1 (V)	Ipa_1 (µA)	Epa_2 (V)	Ipa_2 (µA)
1	0	0.52	1.38	-	-
2	2	0.34	2.45	0.72	10.93
3	4	0.35	2.86	0.75	10.54
4	6	0.35	2.92	0.76	10.07
5	8	0.36	2.99	0.71	9.09
6	10	0.37	3.21	0.70	9.00

Table 3 — CV of p-SC4 with varying concentration of DPA at the scan rate of 50 mV/s

S. No	Concentration of DPA (mL, 10^{-3}mol/L)	Epa_1 (V)	Ipa_1 (µA)	Epa_2 (V)	Ipa_2 (µA)
1	0	0.81	7.16	-	-
2	2	0.67	6.36	0.38	3.65
3	4	0.68	8.65	0.34	3.13
4	6	0.69	10.04	0.33	3.15
5	8	0.72	11.89	0.32	3.17
6	10	0.73	13.14	0.32	3.26

from electrochemical titrations are around 10^{-3} L/mol, whereas the binding constant values obtained from spectrofluorometric titration is around 10^{-4} L/mol. This is due to the competitive binding of counter ions of p-SC4 with DPA[18] However, the fluorescent technique is only considering the fluorescence change from DPA and also it is comparatively sensitive technique than electrochemical techniques. Therefore the binding constant obtained from fluorescence technique is higher than the binding constants obtained from electrochemical techniques.

NMR spectral titration

For easy interpretation purpose, the structure of p-SC4 and DPA with protons labelling are displayed in Fig. S7. The ^{1}H NMR spectrum of DPA in CD_3CN and p-SC4 in D_2O are shown in Fig. S8 and S9. The p-SC4 protons have appeared at 7.3, 3.75 and 1.7 ppm corresponds to aromatic protons (Sc), methylene protons (Sb) and-OH protons (Sa), respectively. Since the aromatic protons are in similar environment for all four phenyl rings. Also all methyl protons are in similar environment. Therefore, these two protons are observed as single peak at 7.3 and 3.75 ppm. Another one signal is for phenolic –OH, where the peak position will vary due to the exchange of protons in water. The DPA protons shows four different peaks at 3.55, 6.91, 7.12 and 7.28 ppm, which are attributed to the amine (-NH) proton (a) and the other three aromatic protons from phenyl ring (b, c & d). The ^{1}H NMR titrations of DPA alone and DPA/p-SC4 mixtures in CD_3CN/D_2O (1:3) is shown in Fig. 6. All the protons of DPA are shifted towards downfield with the incremental addition of p-SC4. The chemical shift value changes are given in Table 4. This is the evidence for the host-guest complexation of DPA with p-SC4 with upper rim binding[56-58,27]. The ROESY technique was used to know the mode of binding between DPA and p-SC4. The ROESY spectrum of DPA with p-SC4 mixture (1:1) in CD_3CN/D_2O is shown in Fig. 7. The amine proton (a) and the aromatic protons (b, c & d) of DPA correlate with the $–CH_2$ protons (Sb) and the aromatic protons (Sc) of p-SC4. There is no correlation observed for the –OH protons (Sa) of p-SC4. Therefore, the binding of DPA with p-SC4 is predominantly at the upper rim.

Computational studies

We modeled three host-guest orientations with DPA and p-SC4, in the first orientation, we placed the DPA molecule horizontally in the cavity of p-SC4 and in the other two orientations the DPA in the vertical

Table 4 — Chemical shift values of the ^{1}H NMR spectral titration of DPA with p-SC4 in CD_3CN/D_2O (1:3)

Proton	DPA	DPA/p-SC4 mixture (1:1)	Change (ppm)
a	3.55	3.91	0.36
b	6.91	7.21	0.30
c	7.12	7.40	0.28
d	7.28	7.57	0.29

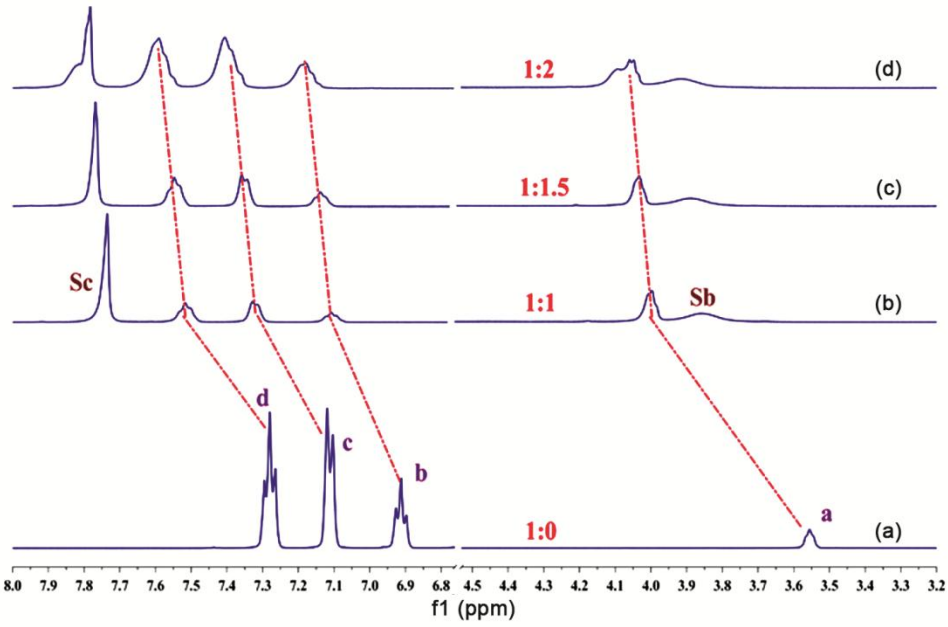

Fig. 6 — ^{1}H NMR spectral titration of (a) DPA (1:0) alone, (b) DPA with p-SC4 in 1:1 ratio, (c) mixture of DPA with p-SC4 in 1:1.5 ratio and (d) is the 1:2 ratio of DPA with p-SC4 in CD_3CN/D_2O (1:3). The solvent peaks are excluded for clarity.

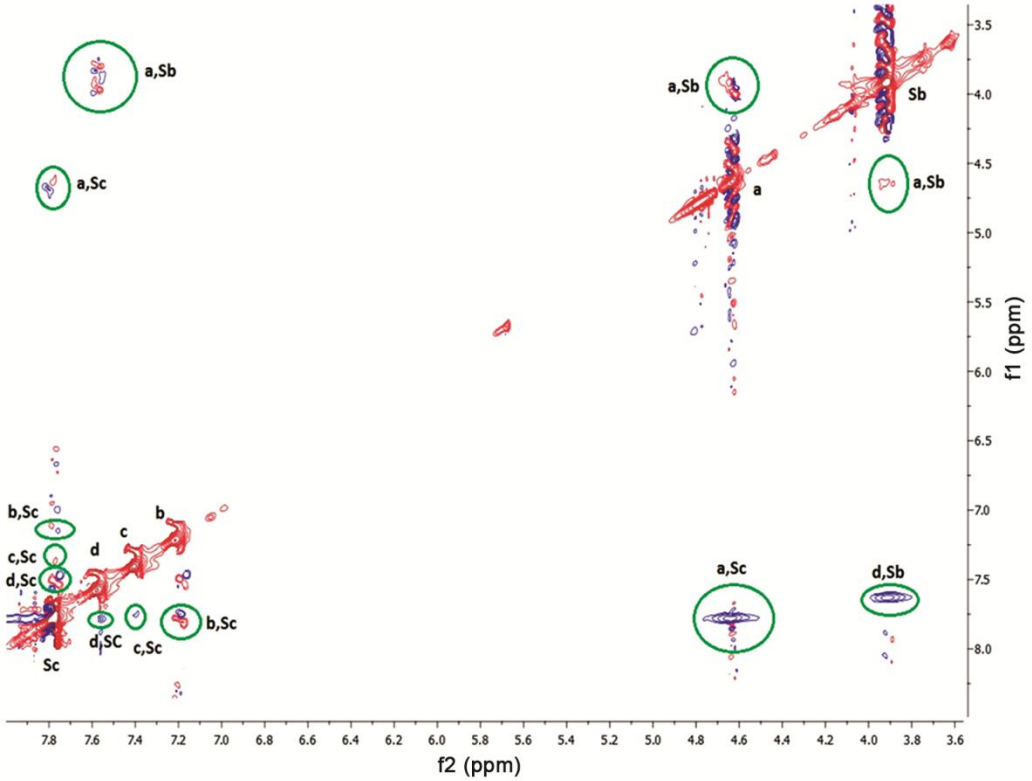

Fig. 7 — ROESY spectrum of mixture of DPA with p-SC4 (1:1) in CD_3CN/D_2O (1:3).

orientation. In the two vertical orientations, the phenyl rings present inside the p-SC4 cavity are perpendicular to each other. The optimized geometries of DPA and p-SC4 are given in Fig. 8. The optimized geometries of the modeled p-SC4-DPA system have been given in Fig. 9. The high complexation energy (-76.94 kJ/mol) of the first model (horizontally placed orientation) indicates the strong binding of DPA with p-SC4 in its horizontal orientation. The calculated complexation energies for the vertical models are -65.06 and -59.16 kJ/mol. The H-bond distance is 2.27, 2.29, and 2.32 Å, respectively for horizontal, vertical-1, and vertical-2 models. The high complexation energy of the horizontal model can be attributed to the shortest H-bond formed between amine hydrogen and oxygen of one of the sulfonate groups of p-SC4 (highlighted in Fig. 9). As the H-bond distance increased, the complexation energy between DPA and p-SC4 decreased. All the complexation energies were corrected for basis set superposition error with counterpoise method[59]. The simulated complexation energies (BSSE corrected and uncorrected), dipole moments of the host-guest complexes were compiled in Table 5. The most stable complex (the first model) is chosen to investigate the

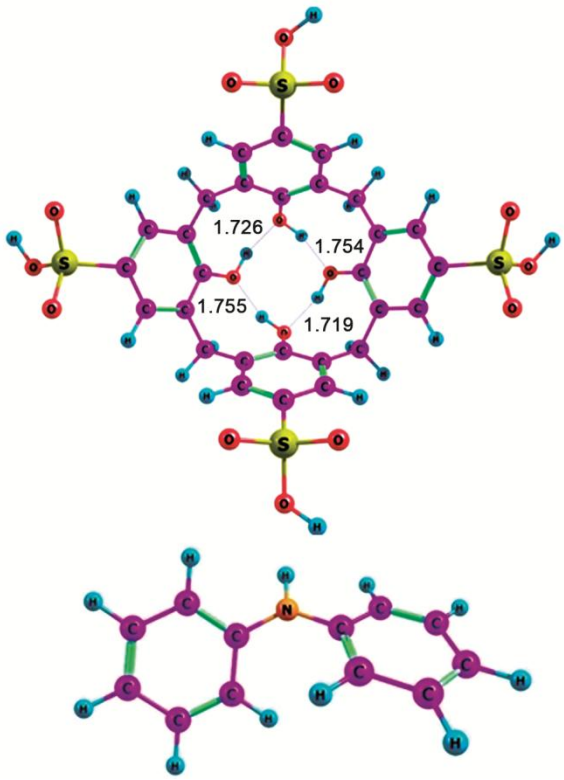

Fig. 8 — The optimized geometries of the p-SC4 (top) and DPA (bottom) obtained at M06-2X/6-31G (d) level of theory.

Table 5 — Calculated complexation energies of DPA with p-SC4 in various orientations

S. No	DPA orientation type	Complexation energy (kJ/mol)	BSSE uncorrected complexation energy (kJ/mol)	Dipole moment (D)
1	Horizontal	-76.94	-116.69	11.81
2	Vertical-1	-65.06	-96.57	13.59
3	Vertical-2	-59.16	-87.07	13.53

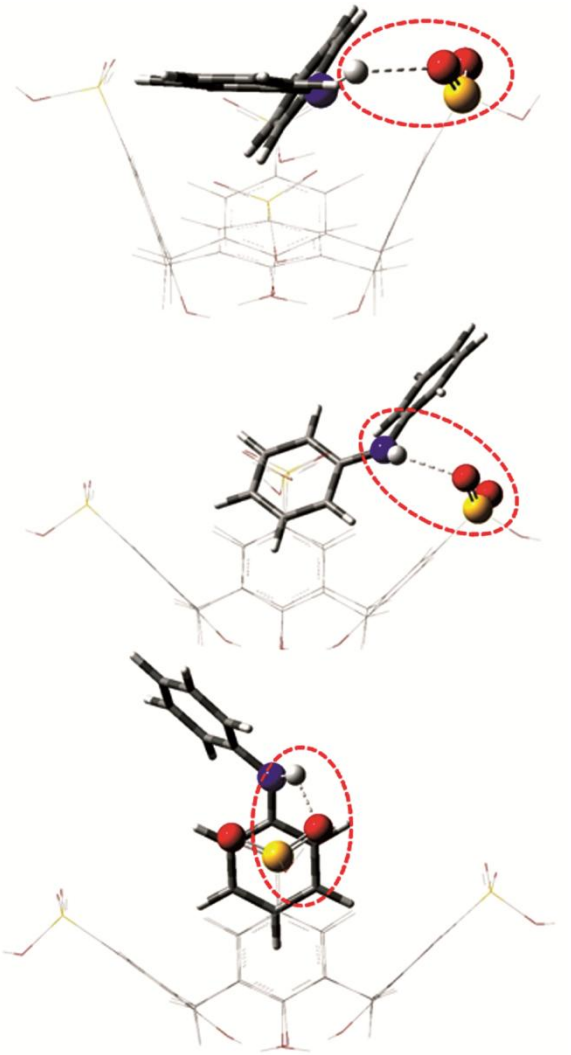

Fig. 9 — The optimized geometries of the DPA with p-SC4 complex in three orientations, horizontal (top), vertical-1 (middle), and vertical-2 (bottom) computed at M06-2X/6-31G(d) level of theory. The hydrogen bonds are encircled with dots.

charge transfer phenomenon. The electron density distribution in the frontier molecular orbitals is given in Fig. 10. In the HOMO, the electron density is localized over DPA and it has been completely transferred to p-SC4 in LUMO, which indicates the charge transfer upon complexation. The binding mode of all the orientations is at the upper rim, which is correlating with the NMR spectral studies.

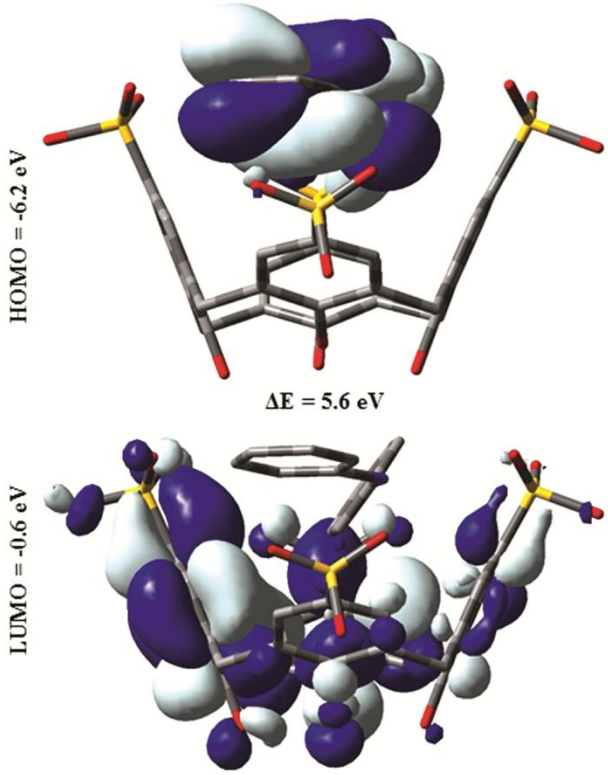

Fig. 10 — Frontier molecular orbitals (HOMO and LUMO) of the most stable host-guest complex computed at M06-2X/6-31G (d) level of theory. Hydrogens are omitted for clarity.

Conclusions

The binding constant value obtained from fluorescence measurement is 1.46×10^4 L/mol, which shows the efficient binding of DPA with p-SC4. The substantial increase in the fluorescence intensity as well as the lifetime of DPA in the presence of p-SC4 is observed due to the binding of DPA with p-SC4. The negative shift in the oxidation potential and increase in the oxidation current of DPA in presence of p-SC4 reveal the complexation between the two components. The binding constant values calculated from cyclic voltammetry are around 10^3 L/mol, express the considerable binding. The theoretical simulations reveal that the complexation of DPA with p-SC4 is stronger when the DPA is placed horizontally in the cavity of p-SC4 with a complexation energy of -76.94 kJ/mol. ^{1}H NMR

spectral titration and the ROESY studies strongly emphasized the upper rim binding of p-SC4.

Supplementary Data

Supplementary data associated with this article are available in the electronic form at http://www.niscair.res.in/jinfo/ijca/IJCA_56A (07) 929-938_SupplData.pdf.

Acknowledgement

This research work was supported by Department of science and Technology (DST INSPIRE) [Project number – IFA14/CH-147], India and Korea Research Fellowship program funded by the Ministry of Science, ICT and Future Planning through the National Research Foundation of Korea (2016H1D3A1936765).

References

1 Chao J, Zhang Y, Fan X, Wang H & Li Y, *Spectrochim Acta A*, 116 (2013) 295.
2 Chao J, Li Z, Liu Y, Zhang Y, Guo Z, Zhang B & Wang X, J *Mol Liq*, 213 (2016) 173.
3 Yang L, Xie X, Cai L, Ran X, Li Y, Yin T, Zhao H & Li C P, *Biosens Bioelect*, 82 (2016) 146.
4 Danjou P E, De Leener G, Cornut D, Moerkerke S, Mameri S, Lascaux A, Wouters J, Brugnara A, Colasson B, Reinaud O & Jabin I, *J Org Chem*, 80 (2015) 5084.
5 Song J, Li H, Chao J, Dong C & Shuang S, *J Incl Phen Macro Chem*, 72 (2012) 389.
6 Baldini L, Sansone F, Casnati A & Ungaro R, *Calixarenes in Molecular Recognition. In: Supramolecular Chemistry*. John Wiley & Sons, Ltd. (2012).
7 Vaze V D & Srivastava A K, *J Pharm Biomed Anal*, 47 (2008) 177.
8 Mokhtari B & Pourabdollah K, *J Incl Phen Macro Chem*, 73 (2012) 1.
9 Costa C, Francisco V, Silva S G, do Vale M L C, García Río L & Marques E F, *Colloids Surf A*, 480 (2015) 71.
10 Qin Z, Guo D S, Gao X N & Liu Y, *Soft Matter*, 10 (2014) 2253.
11 Danylyuk O & Suwinska K, *Chem Commun*, (2009) 5799.
12 Guo D-S, Wang K & Liu Y, *J Incl Phen Macro Chem*, 62 (2008) 1.
13 Muthu Mareeswaran P, Prakash M, Subramanian V & Rajagopal S, *J Phys Org Chem*, 25 (2012) 1217.
14 Patel G & Menon S, *Chem Commun*, (2009) 3563.
15 Bonal C, Israeli Y, Morel J P & Morel Desrosiers N, *J Chem Soc Perkin Trans*, (2001) 1075.
16 Doyle R, Breslin CB, Power O & Rooney A D, *Electroanalysis*, 24 (2012) 293.
17 Muthu Mareeswaran P, Babu E, Sathish V, Kim B, Woo S I & Rajagopal S, *New J Chemistry*, 38 (2014) 1336.
18 Francisco V, Basilio N & García Río L, *J Phys Chem B*, 116 (2012) 5308.
19 Guo D S & Liu Y, *Acc Chem Res*, 47 (2014) 1925.
20 Guo D S, Uzunova V D, Su X, Liu Y& Nau W M, *Chem Sci*, 2 (2011) 1722.
21 Ashwin B C M A, Arulanandu H A B, Muthuramalingam P, Majdi H & Muthu Mareeswaran P, *J Phys Org Chem*, 31 (2018) e3788.
22 Ashwin B C M A, Chitumalla R K, Herculin Arun Baby A, Jang J &, Muthu Mareeswaran P, *J Incl Phen Macro Chem*, 90 (2018) 51.
23 Ashwin B C M A, Vinothini A, Stalin T & Muthu Mareeswaran P, *ChemistrySelect*, 2 (2017) 931.
24 Saravanan C, Senthilkumaran M, Ashwin B C M A, Suresh P & Muthu Mareeswaran P, *J Incl Phen Macro Chem*, 88 (2017) 239.
25 Patil S, Athare S V, Jagtap A, Kodam K M, Gejji S P & Malkhede D D, *RSC Adv*, 6 (2016) 110206.
26 Saravanan C, Ashwin B C M A, Senthilkumaran M & Muthu Mareeswaran P, *ChemistrySelect*, 3 (2018) 2528.
27 Saravanan C, Chitumalla R K, Ashwin B C M A, Senthilkumaran M, Suresh P, Jang J & Muthu Mareeswaran P, *J Lumin*, 196 (2018) 392.
28 Ashwin B C M A, Saravanan C, Senthilkumaran M, Sumathi R, Suresh P & Muthu Mareeswaran P, *Supramol Chem*, 30 (2018) 32.
29 Senthilkumaran M, Maruthanayagam K, Vigneshkumar G, Chitumalla R K, Jang J & Muthu Mareeswaran P, *J Fluoresc*, 27 (2017) 2159.
30 Madasamy K, Gopi S, Kumaran M S, Radhakrishnan S, Velayutham D, Muthu Mareeswaran P & Kathiresan M, *ChemistrySelect*, 2 (2017) 1175.
31 Li H, Guan A, Huang G, Liu CL, Li Z, Xie Y & Lan J, *Bioorg MedChem*, 24 (2016) 453.
32 Saad B, Haniff N H, Idiris Saleh M, Hasani Hashim N, Abu A & Ali N, *Food Chem*, 84 (2004) 313.
33 Drzyzga O, *Chemosphere*, 53 (2003) 809.
34 Li S X, Wei D, Mak N-K, Cai Z, Xu X-R, Li H-B & Jiang Y, *J Hazard Mater*, 164 (2009) 26.
35 Poliak P, Vagánek A, Lukeš V & Klein E, *Poly Degrad Stability*, 114 (2015) 37.
36 Sur D, Purkayastha P & Chattopadhyay N, *J Photochem Photobiol A*, 134 (2000) 17.
37 Srinivasan K, Kayalvizhi K, Sivakumar K & Stalin T, *Spectrochim Acta A*, 79 (2011) 169.
38 Ganesan S, Muthuraaman B, Mathew V, Madhavan J, Maruthamuthu P& Austin Suthanthiraraj S, *Solar Energy Mater Solar Cells*, 92 (2008) 1718.
39 Rajamohan R & Swaminathan M, *Spectrochim Acta A*, 83 (2011) 207.
40 Enoch I V M V & Swaminathan M, *J Chem Res*, 8 (2006) 523.
41 Enoch I V M V & Swaminathan M, *J Lumin*, 127 (2007) 713.
42 Xiong D, Chen M & Li H, *Chem Commun*, (2008) 880.
43 Lakowicz J R, *Principles of Fluorescence Spectroscopy*. (2007) Springer US,
44 Paramasivaganesh K, Srinivasan K, Manivel A, Anandan S, Sivakumar K, Radhakrishnan S & Stalin T, *J Mol Struct*, 1048 (2013) 399.
45 Frisch M J, Trucks G W, Schlegel H B, Scuseria G E, Robb M A, Cheeseman J R, Scalmani G, Barone V, Mennucci B, Petersson GA, Nakatsuji H, Caricato M, Li X, Hratchian HP, Izmaylov A F, Bloino J, Zheng G, Sonnenberg J L, Hada M, Ehara M, Toyota K, Fukuda R, Hasegawa J, Ishida M, Nakajima T, Honda Y, Kitao O, Nakai H, Vreven T, Montgomery J A, Peralta JE, Ogliaro F, Bearpark M,

Heyd J J, Brothers E, Kudin K N, Staroverov V N, Kobayashi R, Normand J, Raghavachari K, Rendell A, Burant J C, Iyengar SS, Tomasi J, Cossi M, Rega N, Millam J M, Klene M, Knox J E, Cross J B, Bakken V, Adamo C, Jaramillo J, Gomperts R, Stratmann R E, Yazyev O, Austin A J, Cammi R, Pomelli C, Ochterski J W, Martin R L, Morokuma K, Zakrzewski V G, Voth G A, Salvador P, Dannenberg J J, Dapprich S, Daniels A D, Farkas, Foresman J B, Ortiz J V, Cioslowski J & Fox D J, *Gaussian 09, Revision B.01*.(2009)Wallingford CT.

46 Zhao Y & Truhlar D G, *Theoretical Chem Acc*, 120 (2008) 215.

47 Bakirci H, Koner A L & Nau W M, *Chem Commun*, (2005) 5411.

48 Francisco V, Basílio N & GarcíaRío L, *J Phys Chem B*, 118 (2014) 4710.

49 Pessêgo M, Basílio N, Muñiz M C & GarcíaRío L, *Org Biomol Chem*, 14 (2016) 6442.

50 Santhosh P, Sankarasubramanian M, Thanneermalai M, Gopalan A & Vasudevan T, *Mater Chem Phys*, 85 (2004) 316.

51 Yang H & Bard A J, *J Electroanal Chem Inter Electrochem*, 306 (1991) 87.

52 Wen T C, Chen J B & Gopalan A, *Mater Lett*, 57 (2002) 280.

53 Inzelt G, J Solid State *Electrochem*, 6 (2002) 265.

54 Diao G & Zhou W, *J Electroanal Chem*, 567 (2004) 325.

55 Diao G & Liu Y, *Electroanalysis*, 17 (2005) 1279.

56 Kalyani V S & Malkhede DD, *J Incl Phen Macro Chem*, 87 (2017) 179.

57 Fernandes C M, Carvalho R A, Pereira da Costa S & Veiga F J B, *Euro J Pharm Sci*, 18 (2003) 285.

58 Senthilkumaran M, Chitumalla RK, Vigneshkumar G, Rajkumar E, Muthu Mareeswaran P & Jang J, *J Incl Phen Macro Chem*, 91 (2018) 161.

59 Boys S F & Bernardi F, *Mol Phys*, 19 (1970) 553.